



HAL
open science

Iron(II)-Catalyzed Activation of Si–N and Si–O Bonds Using Hydroboranes

Mirela A. Farcaș-Johnson, Danila Gasperini, Andrew K. King, Sakshi Mohan,
Adam N. Barrett, Samantha Lau, Mary F. Mahon, Yann Sarazin, Sara H.
Kyne, Ruth L. Webster

► **To cite this version:**

Mirela A. Farcaș-Johnson, Danila Gasperini, Andrew K. King, Sakshi Mohan, Adam N. Barrett, et al.. Iron(II)-Catalyzed Activation of Si–N and Si–O Bonds Using Hydroboranes. *Organometallics*, 2023, 42 (20), pp.3013-3024. 10.1021/acs.organomet.3c00339 . hal-04261558

HAL Id: hal-04261558

<https://hal.science/hal-04261558v1>

Submitted on 3 Nov 2023

HAL is a multi-disciplinary open access archive for the deposit and dissemination of scientific research documents, whether they are published or not. The documents may come from teaching and research institutions in France or abroad, or from public or private research centers.

L'archive ouverte pluridisciplinaire **HAL**, est destinée au dépôt et à la diffusion de documents scientifiques de niveau recherche, publiés ou non, émanant des établissements d'enseignement et de recherche français ou étrangers, des laboratoires publics ou privés.

Iron(II) Catalyzed Activation of Si–N and Si–O Bonds Using Hydroboranes

Mirela A. Farcaş-Johnson,^{†‡} Danila Gasperini,[†] Andrew K. King,[†] Sakshi Mohan,^ψ Adam N. Barrett,[†] Samantha Lau,[†] Mary F. Mahon,[†] Yann Sarazin,^ψ Sara H. Kyne,^{‡*} Ruth L. Webster^{†*}

[†] Department of Chemistry, University of Bath, Claverton Down, Bath, United Kingdom, BA2 7AY.

[‡] School of Chemistry, Faculty of Science, University of New South Wales, Sydney, NSW 2052, Australia

^ψ Institut des Sciences Chimiques de Rennes, Université de Rennes, Campus de Beaulieu, 35042 Rennes, France

Supporting Information Placeholder

ABSTRACT: We report the activation and functionalization of Si–N bonds with pinacol borane catalyzed by a three-coordinate iron(II) β -diketimate complex. The reactions proceed via mild activation of silazanes to yield useful hydrosilanes and aminoboranes. The reaction is thoroughly studied by kinetic analysis, along with a detailed investigation of decomposition pathways using catecholborane as an analogue of the pinacol borane used in catalysis. We have extended the methodology to develop a polycarbosilazane depolymerization strategy, which generates hydrosilane quantitatively, along with complete conversion to the Bpin-protected diamine. The analogous Si–O bond cleavage can also be achieved with heating, using silyl ether starting materials to generate hydrosilane and alkoxyborane products. Depolymerization of poly(silyl ether)s using our strategy successfully converts the polymer to 90% of Bpin-protected alcohols.

1. INTRODUCTION

The advancement of silicon chemistry is one of the most prolific in modern chemistry with ubiquitous applications in commercial products and materials.¹ Furthermore there has been the extensive development of silicon compounds as protecting groups in organic synthesis,^{2,4} and as nucleophilic reagents in cross-coupling reactions with organohalides and pseudohalides.³ Beyond this, the range and ease of access to organosilicon oligomers and polymers have improved to allow production and study of new materials with properties that complement or match those of petroleum-derived plastics.^{6–10, 11–12}

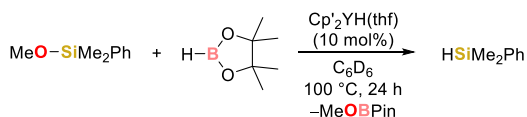
Silyl ether Si–O bonds are largely considered unreactive and serve as useful alcohol protecting groups. The cleavage of these bonds is often achieved by treatment with acids or fluoride ion sources where the reaction is driven by the formation of a strong and chemically inert Si–F bond.¹³ As a consequence, there are limited reports of Si–O bond activation. One recent example includes the reduction of silyl ether monomers using pinacol borane (HBpin) in the presence of a metallocene-type yttrium catalyst. The procedure was applied to methoxydimethyl(phenyl)silane, and required 100 °C for 24 h with 10 mol% catalyst loading to release the synthetically useful dimethylphenylsilane (Scheme 1a).¹⁴ Enthaler and co-workers demonstrated several air-stable routes to activate polydimethylsiloxane (PDMS) catalyzed by readily available transition-metal salts to form Si–F and Si–Cl monomers (Scheme 1b).^{15–17} Similar procedures have also been used to afford various silyl ether monomers. (Scheme 1b).¹⁶

Silazane Si–N bond activation has been less widely studied, potentially due to their greater rate of hydrolysis compared to silyl ethers.^{18–19} Other than hydrolysis or alcoholysis to generate Si–O bonds,²⁰ few reactions of silazanes have been studied in detail.²¹ Existing examples generally involve reaction with stoichiometric halide displacement reagents such as chloroboranes, to form strong Si–Cl bonds. Although the release of chlorosilane was not the focus of the work, Helten employed this approach in the condensation of *N*-trimethylsilylaniline and dichloro(mesityl)borane to afford a polymer consisting of alternating NBN and *p*-phenylene units and Me₃SiCl under relatively mild

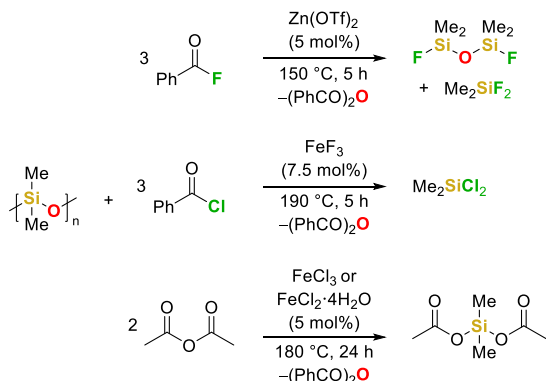
conditions (Scheme 1c).²² Few examples to generate hydrosilanes have been reported, particularly employing milder reducing agents. Further stoichiometric Si–N activation examples include the work of Wrackmeyer, where 9-BBN was reacted with silazanes (such as hexamethyldisilazane, HMDS) neat at 120–130 °C for up to 5 h to generate tertiary silane and amine-borasilane products (Scheme 1d).²³ Although there was a limited scope, selective cleavage of Si–N over N–H bonds was observed, however complete cleavage of all Si–N bonds in the substrates was not explored.

There is a growing focus on developing catalytic approaches to activate Si–heteroatom bonds. While the catalytic activation of Si–Si,^{24–25} Si–B^{26–28} and Si–P²⁹ has been explored, to the best of our knowledge there are no examples of catalytic Si–N bond activation, not least by an iron pre-catalyst. We have previously demonstrated the use of iron β -diketimate complexes in efficient heterodehydrocoupling reactions^{30–33} and during these studies, our mechanistic investigations showed that the Si–N bond forming step was fast and reversible (Scheme 1e). This led us to question whether we could specifically target a Si–N bond activation process, which could be used to effect a poly(silazane) depolymerization strategy. If successful, this method would offer a more controlled route to Si–N bond cleavage, rather than by simple hydrolysis, giving access to higher value products, for example hydrosilane and aminoborane compared to silanol and amine.

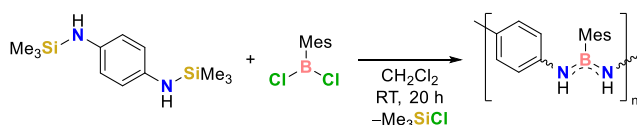
a) O-Si (Nakajima)



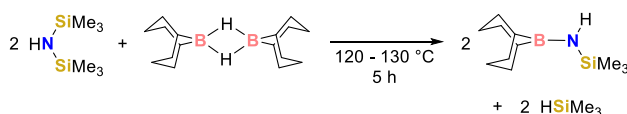
b) O-Si polymers (Enthaler)



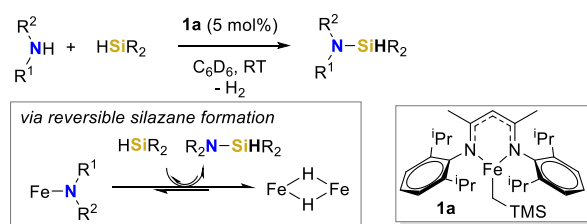
c) N-Si (Helten)



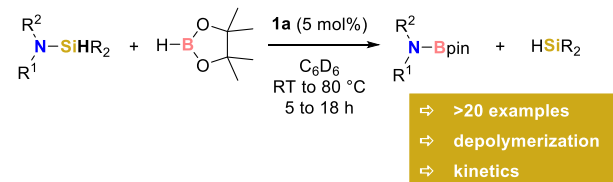
d) N-Si (Wrackmeyer)



e) Our Previous Work



f) This Work - exploiting reversibility



Scheme 1. Examples of Si-X bond activation.

We herein report a scarcely studied catalytic Si-N bond activation using iron(II) β -diketiminate pre-catalyst **1a** to generate hydrosilanes and aminoboranes from both monomeric and polymeric substrates (Scheme 1f). We also present a postulated mechanism supported by kinetic studies.

2. RESULTS AND DISCUSSION

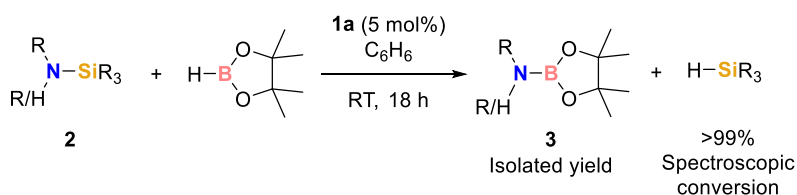
2.1 Reaction Scope

Silazanes with a secondary substituted silicon atom (**2a-2t**), were reacted with HBpin with 5 to 10 mol% of pre-catalyst **1a**;³⁴ the reaction typically operates well at RT but is limited by substituents both on nitrogen and silicon (Table 1). A generally observed trend allowed us to differentiate the reactivity of aryl and alkyl substituted silazanes. In fact, when reacting silazanes containing secondary or primary amines with *alkyl* substituents, such as **2a** to **2e** (Table 1, Entries 1 to 5), the reaction proceeded smoothly and quickly (in as little as 5 h, with 5 mol% **1a**) to give products **3a-e** in good to excellent yields (67–92% isolated yield). By increasing the steric bulk on the alkyl chain, a slight increase in temperature (to 50 °C) is required to ensure full conversion of **2f** to generate **3f** in 82% isolated yield (Entry 6). Pleasingly **3g** forms chemoselectively from **2g** at RT with no trace of Si-O bond activation (>99% spectroscopic conversion, Entry 7). Unfortunately, in the case of silazane **2h** with bulkier trityl substituents does not undergo reaction to give **3h** (Entry 8). When silazane reagents **2i-2l**, which have aniline or tetrahydroquinoline substituents, are reacted with HBpin, harsher conditions are required (pre-catalyst **1a** loading up to 10 mol% and temperatures up to 80 °C, Entries 9 to 12). Next, we probed the reaction by varying the silane substitution, and observe full conversion of **2o** into aminoborane **3a** (65% isolated yield), albeit requiring a longer reaction time to reach full conversion (18 h from **2m**, Entry 13, versus 5 h from **2a**, Entry 1). Higher temperatures (50 °C) are required when synthesizing **3e**, starting from **2n** (67% isolated yield, Entry 14), and **3j** starting from silazane **2q** (>99% spectroscopic conversion, Entry 15). When more challenging silazanes are used, such as **2p** to **2r**, which have two Si-N bonds, the reaction requires 10 mol% of **1a** and heating to 50 °C to allow full conversion to give **3a**, **3e** and **3l** in >99, 50 and 98% isolated yields respectively (Entries 16, 17 and 18).

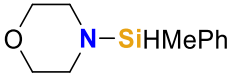
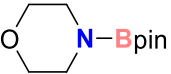

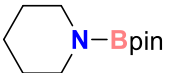

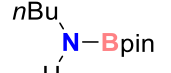

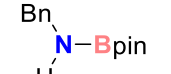

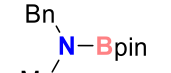
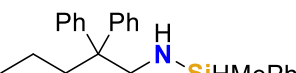
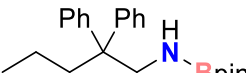
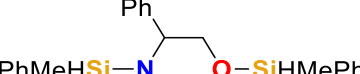
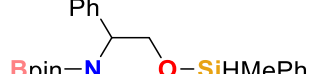
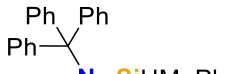
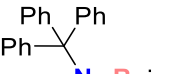
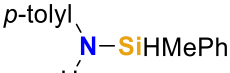
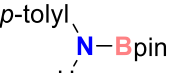

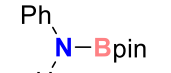

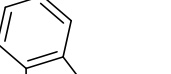

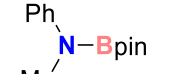
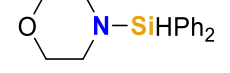
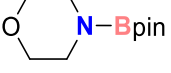

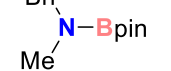
It is worth noting that **2a** reacts with HBpin in the absence of **1a** after 48 h at RT. However, only 38% spectroscopic conversion to **3a** is observed under these conditions along with potential onward decomposition of aminoborane **3a** (see SI, page S43 for details). Clearly the presence of the iron pre-catalyst (**1a**) is necessary and important for clean and full conversion of silazanes. This is also borne out for the Si-O bond cleavage in silyl ethers (*vide infra*).

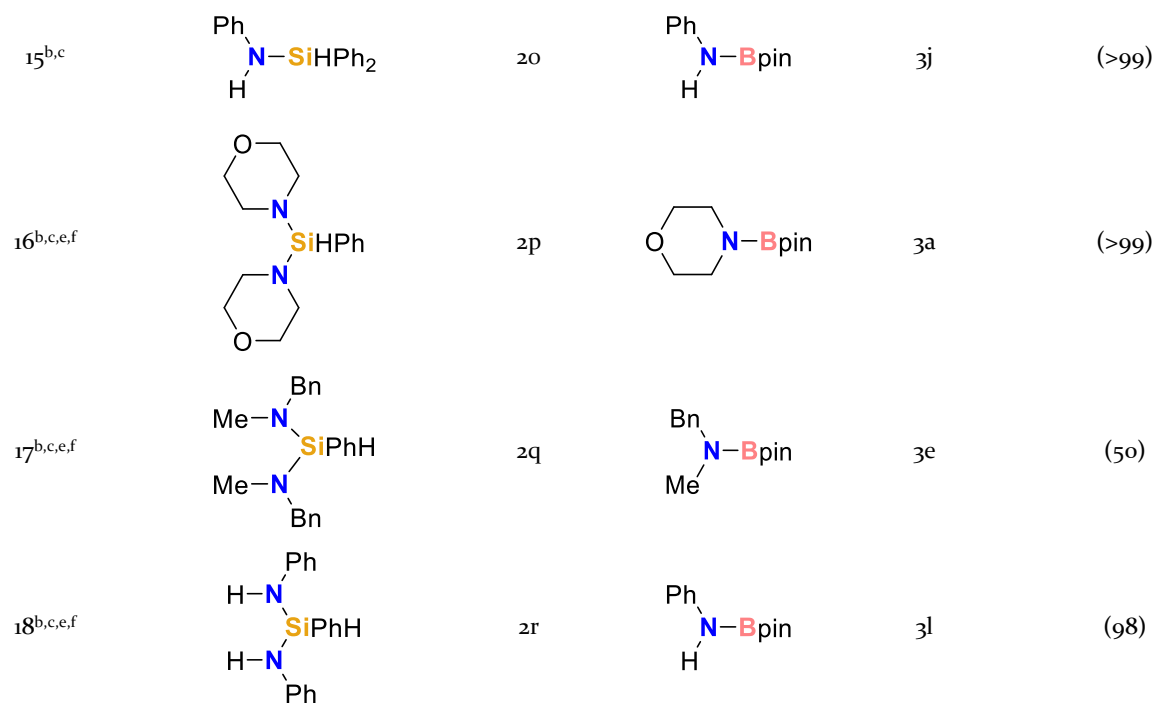
Unfortunately, depolymerization of a commercially available poly(silazane) was unsuccessful; commercially available Durazane 1800 (Figure 1a, see SI pages S45 to S60 experimental studies) underwent competitive cross-linking under all reaction conditions tested, generating polymer with narrower M_w and \mathcal{D} , but with no discernable generation of monomers.

Table 1. Scope of silazane substrates undergoing Si-N activation.



Entry	Starting Material	Aminoborane Product	Isolated Yield, % (Spectroscopic Conversion, %)
-------	-------------------	---------------------	--

1 ^a		2a		3a	80
2 ^a		2b		3b	75
3		2c		3c	92
4		2d		3d	78
5		2e		3e	67
6 ^b		2f		3f	82
7		2g		3g	(>99)
8		2h		3h	0
9 ^c		2i		3i	78
10 ^c		2j		3j	85
11 ^d		2k		3k	72
12 ^d		2l		3l	82
13		2m		3a	65
14 ^c		2n		3e	67



Reaction conditions: **1a** (5 mol%), **2** (0.5 mmol, 1 equiv.), HBpin (0.5 mmol, 1 equiv.), C₆D₆ (0.5 mL), RT, 18 h. Isolated yield reported unless noted; spectroscopic conversion calculated by ¹H NMR spectroscopy based on loss of Si-H in compounds **2** and concomitant growth of Si-H in hydrosilane (1:1 ratio). ^a5 h; ^b50 °C; ^c10 mol% **1a**; ^d80 °C; ^e1 mmol HBpin; ^fFor spectroscopic conversion of bis-aminosilane substrates (**2p**, **2q** and **2r**) one mole of hydrosilane is obtained for every two moles of aminoborane product e.g. Entry 17, **3e** = 50% spectroscopic conversion, H₃SiPh = 25% spectroscopic conversion.

Clearly, we needed to target a polymer that is not prone to competing side-reactions. We thus employed polycarbosilazanes³⁵ in depolymerization. We employed cyclic polymer (**P1**) with *M_n* = 17.5 kDa (by DOSY NMR analysis) and linear polymer (**P2**, Figure 1b, top, purple) with *M_n* = 3.7 kDa (by DOSY, Diffusion-Ordered Spectroscopy, NMR analysis). Both polymers behave similarly under a slightly re-optimized set of desilylation conditions: no depolymerization is observed when the sample is heated for 3 days at 80 °C (Figure 1b, purple spectrum, top). No depolymerization is observed when this is repeated in the presence of 3 equiv. HBpin per polymer repeat unit (turquoise spectrum). However, in the presence of **1a** at RT the immediate release of H₂ is observed as free NH₂ bonds undergo dehydrocoupling with

HBpin (Figure 1b, green spectrum). However, shaking this reaction at RT for 3 days leads to a limited amount of silane release (<10% H₂SiPh₂ spectroscopic yield, green spectrum). When the reaction is repeated (5 mol% **1a** relative to mmol of **P1/P2** used, 3 equiv. HBpin relative to polymer repeat unit, 80 °C, 2 days) there is almost complete loss of polymer signals from the ¹H NMR signal, H₂SiPh₂ is observed in >99% spectroscopic yield (measured against hexamethylbenzene as an internal standard) and the formation of aminoborane product (>99% spectroscopic yield, maroon spectrum, Figure 1, bottom) is clearly observed. The presence of the Bpin-protected *para*-xylylenediamine is confirmed by high resolution LC-QTOF (Liquid Chromatography Quadrupole Time-of-Flight) mass spectrometry.

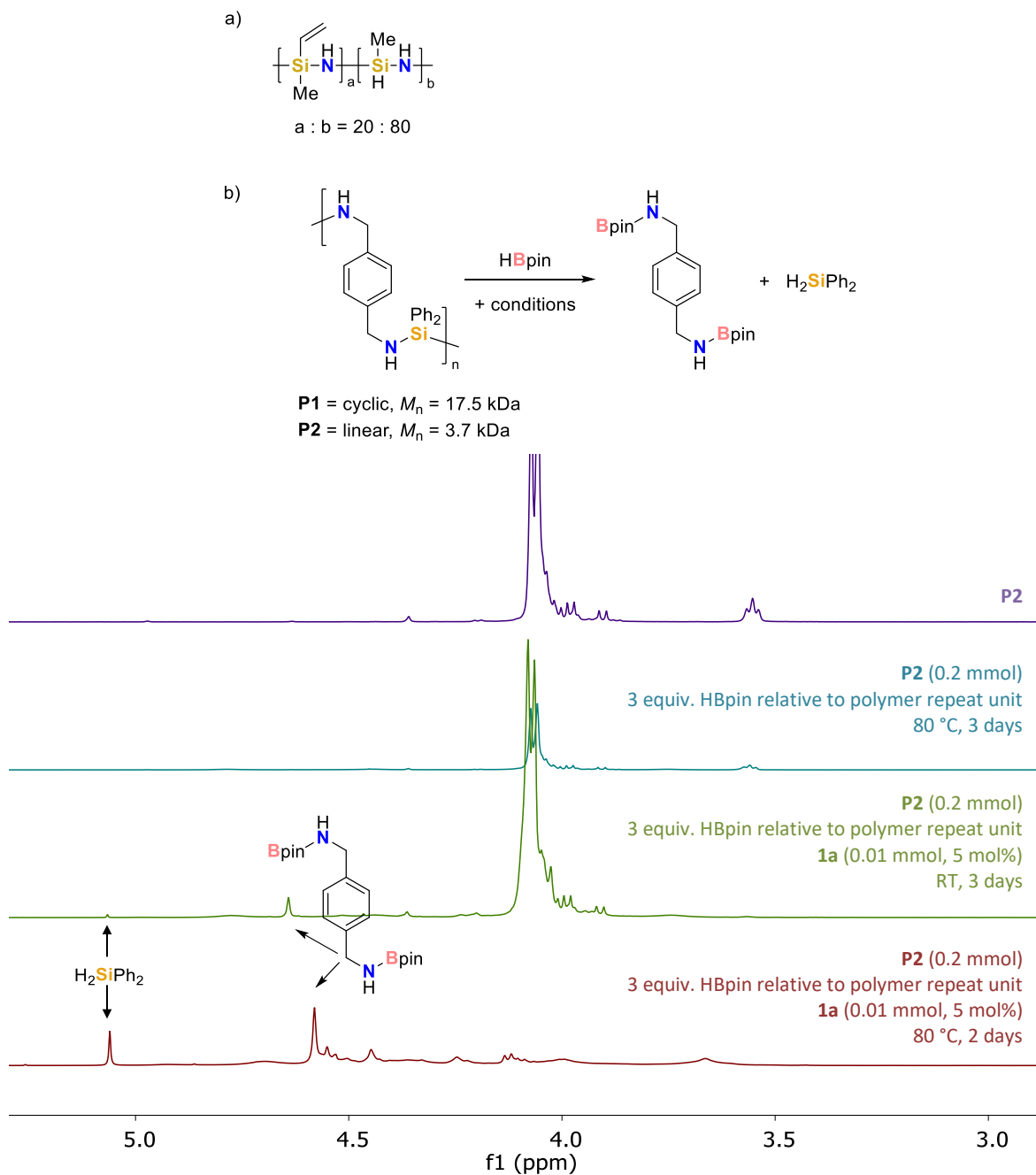


Figure 2. a) Durazane 1800 polymer tested in depolymerization reactions. b) Depolymerization reaction undertaken using **P1** and **P2** and 1H NMR spectra showing depolymerization results for **P2**.

Next, we probed the viability of silyl ether activation. More forcing conditions are required (70 °C compared to RT with silazanes) and this is likely due to the competing bond strengths, where cleavage of a strong Si–O bond is not readily outweighed by the formation of a B–O bond. However, we are pleased to report that a selection of aliphatic and benzylic silyl ethers (**4a–d**) undergo desilylation in the presence of **1a** (5 mol%) to give **5a–d** respectively in excellent isolated yields (Table 2). Unfortunately, phenoxysilane **4e** does not undergo Si–O bond activation (Entry 5). This is perhaps unsurprising considering our previous studies on dehydrocoupling, where **1a** was unable to catalyze the dehydrocoupling of phenol and hydrosilanes.³³ When commercially available siloxanes (**4f** and **4g**, Entries 6 and 7) were subjected to **1a** (2.5 mol%) and HBpin (1 equiv.), moderate conversion to

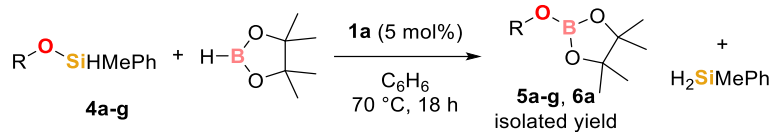
5f and **5g** respectively were observed. **4g** also underwent hydroboration of the alkene (27% conversion to hydroborated product) indicating that our current conditions may not be sufficiently selective in cases where competitive hydroboration reactions may occur. **2g** undergoes complete bond activation, cleaving both the Si–N and Si–O forming the N–Bpin/O–Bpin product (**6a**) along with two equivalents of $H_2SiMePh$ (Entry 8).

Poly(silyl ether) **P3** was synthesized according to our previously reported method.³⁶ Following a short optimization procedure for the depolymerization of **P3**, we find that in the presence of **1a** (5 mol%) at 80 °C, after 18 h, a 90% reduction in M_n relative to the initial polymer M_n is achieved (data obtained from GPC analysis), Scheme 4. The same conditions were also applied to poly(silyl ether) **P4** which also

shows a 90% reduction in M_n . Free MePhSiH₂ is observed by ¹H and ²⁹Si NMR spectroscopy, but unlike the depolymerization of **P1** and **P2**, some polymer is clearly visible in the NMR spectra and complete conversion to free silane is not observed (see SI, pages S64 to S70 for de-

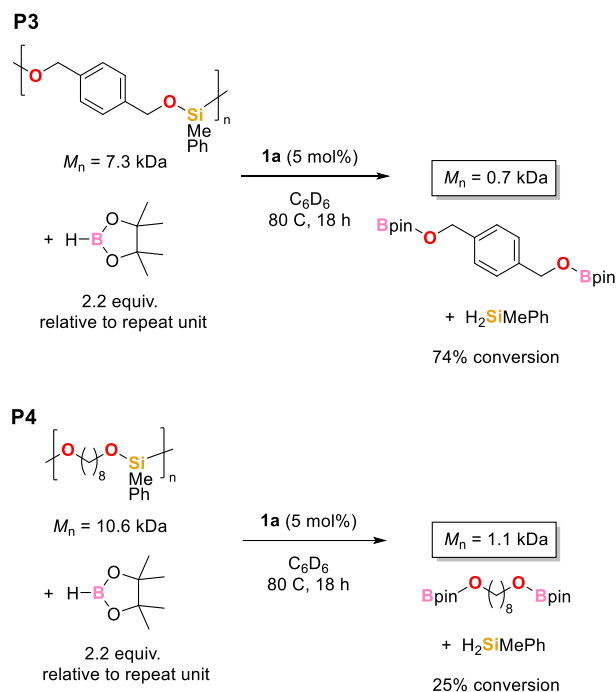
tails). Nonetheless, these data confirm that our desilylation conditions are suitable for depolymerization of poly(silazane)s and poly(silyl ether)s. Unfortunately, commercially available poly(dimethylsiloxane) showed little evidence of depolymerization using under our depolymerization conditions based on ¹H NMR spectroscopic analysis.

Table 2. Scope of silyl ether substrates undergoing Si–O activation.



Entry	Starting Material		Product		Isolated Yield, % (Spectroscopic Conversion, %)
1		4a		5a	81
2		4b		5b	86
3		4c		5c	83
4		4d		5d	>99
5		4e		5e	0
6 ^a		4f		5f	(33)
7 ^a		4g		5g	(27)
8 ^b		2g		6a	67

Reaction conditions: **1a** (5 mol%), **4** or **2g** (0.5 mmol, 1 equiv.), HBpin (0.5 mmol, 1 equiv.), 70 °C, 18 h, C₆D₆. ^a**1a** (2.5 mol%), 80 °C; ^b1 mmol HBpin. Spectroscopic conversion calculated by ¹H NMR spectroscopy based on loss of Si–H in compounds **4** and concomitant growth of Si–H in hydrosilane (1:1 ratio).



Scheme 4. Poly(silyl ether)s depolymerized using **1a** and HBpin. ¹H NMR spectroscopic conversion from polymer SiMe to H₂SiMePh products reported.

2.2 Mechanistic Analysis

Kinetic studies were performed using the morpholine containing **2a** as a model compound and reacting with HBpin (see SI pages S14 to S31 for details). Data obtained by varying pre-catalyst **1a** loading suggest a clear first order dependence on **1a**. A first order dependence is also observed when varying the concentration of silazane (**2a**) and HBpin starting materials (see SI pages S17 to S23). The ¹H NMR spectra of the catalytic reaction shows the immediate appearance (from the first reaction point at $t = 5$ min) of the iron hydride species **1b** [((β -diketiminato)FeH)₂], see SI, page S4, for synthetic procedure. The hydride dimer is present throughout catalysis indicating that this is a catalyst resting state. Kinetic analysis shows the reaction is half-order in **1b** indicating that this dimer splits into two active monomers during the catalytic cycle. Catalysis with 5 mol% **1a** takes approximately 15 minutes to generate **3a** from the reaction of **2a** and HBpin, whereas this initiation period is reduced to approximately 7 minutes when **1b** is employed. Reaction of **1a** with morpholine (i.e. the intermediate formed following cleavage of the Si–N bond, *vide infra*) and recrystallization in pentane at -30 °C gives deep red crystals of **1c-macrocycle**, isolated in 82% yield. Subsequent analysis by single crystal X-ray diffraction shows the iron-morpholine complex crystallizes as a hexamer (Figure 2). The morpholine units bridge the iron centres *via* dative interactions with the oxygen atoms at alternating Fe–N and Fe–O bond distances of 1.894(3) and 2.249(3) Å respectively. The coordination geometry about the iron centres show distortions from both trigonal pyramidal and tetrahedral geometries; the three N–Fe–O angles around each iron centre have a mean of 101.26°. The iron centres of **1c** are equivalent in the solid state, exhibiting a 6-fold pseudo-symmetry axis with the morpholine-oxygen atoms situated at each of the axial positions of the iron atoms. The angles between adjacent iron centres are therefore all equal. The hexamer appears to dissociate in solution; DOSY NMR analysis in C₆D₆ gives signals with diffusion coefficients between 8.98×10^{-10} and 9.07×10^{-10} m² s⁻¹, which correspond to an estimated molecular weight in solution between 455 and 464 g mol⁻¹, see SI Figure S61.³⁷ These values suggest that iron amido **1c** is mononuclear in solution (expected molecular weight of **1c-macrocycle** = 3357.7 g mol⁻¹).

When employed as a catalyst, the reaction is first order in **1c** and the reaction profile is similar to that using **1a**, indicating that **1c** could be an on-cycle species (see SI pages S25 and S26). Catalysis with 5 mol% **1c** shows **3a** forming from **2a** and HBpin within 5 minutes of the reaction starting.

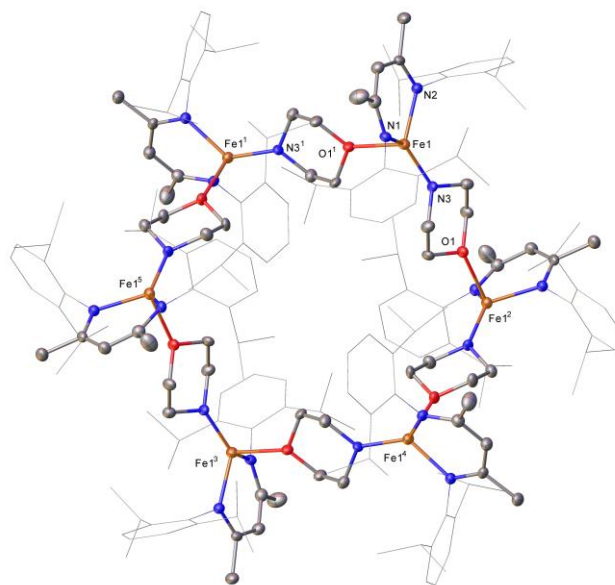


Figure 2. Molecular structure of **1c-macrocycle** (CCDC 1962467). Ellipsoids are represented at 30% probability. Hydrogen atoms have been omitted and the β -diketiminato substituents have been represented in wireframe view, for clarity. Symmetry operations: $1-z, 1-x, -y$; $2-1-y, -z, 1-x$; $3-2-x, -y, -z$; $4+1+z, -1+x, y$; $5+1+y, z, -1+x$.

The kinetic profile for Si–N bond activation of **2a** using DBpin *versus* HBpin gives a primary kinetic isotope effect (KIE) of 1.85 ± 0.04 (see SI pages S38 to S41 for details). The low KIE is in line with a potential non-linear transition state.³⁸ It may also indicate that the rate-limiting step is one that involves H–B bond cleavage. However, when we undertook further labeling studies, these simply acted to highlight that there is an aspect of reversibility in the catalytic cycle, which is in line with our previously reported findings during dehydrocoupling catalysis (see Scheme 1d). For example, silazane with 23% Si–D incorporation (PhDN–Si(H/D)MePh, **2j-d**, see SI pages S32 to S35) undergoes desilylation generating PhDN–Bpin (**3j-d**), H₂SiMePh, HDSiMePh along with unreacted HBpin and some DBpin (indicating reversibility). When proteo-substrate **2a** is reacted under catalytic conditions with DBpin (0.75 equiv.) and analyzed at the point of 69% conversion to **3a**, H₂SiMePh and HDSiMePh are observed spectroscopically (see SI pages S35 to S37), again, indicating reversibility within the catalytic cycle.

Eyring analysis using **1a** gives $\Delta S^\ddagger = -8.1 \pm 0.1$ cal/mol/K, $\Delta H^\ddagger = 4.9 \pm 0.5$ kcal/mol, while Arrhenius analysis gives E_a 23.1 ± 0.2 kJ/mol (see SI pages S28 to S31 for details). These data support the facile nature of the reaction and the mild conditions needed for catalytic turnover, with the low enthalpy and negative entropy values being associated with a relatively ordered transition state.

Attempts to prepare other potential iron-containing intermediates failed. For example, a stoichiometric reaction of **1b**, **2a** and HBpin at RT, followed by crystallization at -78 °C over several days gave bridged BH₂-dimer, **1d** (Figure 3). This is clearly an endpoint in catalysis and although hydridic in nature, this species is not a competent catalyst: it converts **2a** to **3a** five times slower than pre-catalyst **1a** (k_{obs} 1.55×10^{-4} with **1a** *versus* 3.38×10^{-5} mmol⁻¹dm⁻³s⁻¹ with **1d**).

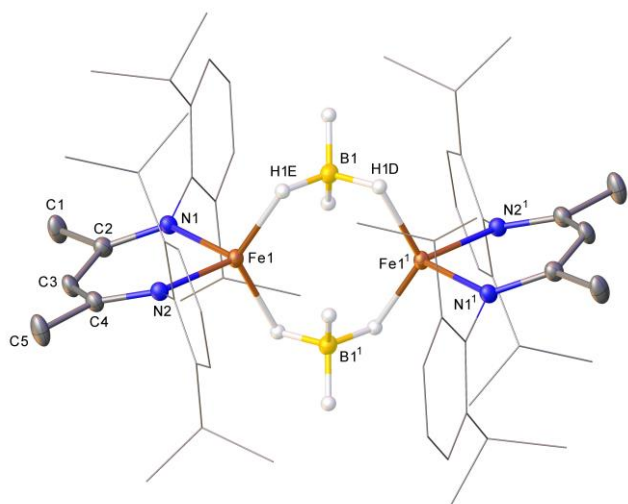
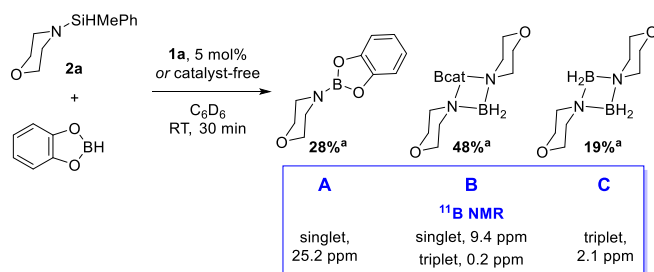


Figure 3. Molecular structure of **1d** (CCDC 2263642). Ellipsoids are represented at 30% probability. Hydrogen atoms, except for those which are bound to boron, have been omitted for clarity and the BDI substituents have been represented in wireframe view, also for clarity. Symmetry operations: $1-x$, $1-y$, $1-z$.

Our reaction optimization studies indicated that catechol borane (HBcat) is a less reactive reagent for Si–N bond activation compared to HBpin. We therefore postulated that this might give us a better opportunity to isolate analogues of likely reactive intermediates. A reaction of **2a**, HBcat and **1a** (5 mol%), shows the immediate formation of three species (**A–C**) after five minutes at RT, with a visible color change of the solution from dark brown to bright orange. Over the course of 24 h **B** remains a minor component of the reaction mixture, while **A** and **C** increase (approximately 3 : 1 : 0.8 ratio of **A** : **B** : **C** after 30 mins, then 15 : 1 : 6 after 24 h).

Using ^{11}B NMR spectroscopy, we can assign these species as aminoborane (**A**, singlet at 25.2 ppm),³⁹ a partial decomposition species (**B**) containing two different boron centers (the ^{11}B NMR spectrum displays a sharp singlet at 9.4 ppm and a triplet at 0.2 ppm), and complete decomposition species **C** (triplet at 2.1 ppm),⁴⁰ Scheme 5.



Scheme 5. Decomposition species observed in the reaction of **2a** with HBcat. Reaction conditions: **1a** (0 or 5 mol%), **2a** (0.2 mmol, 1 equiv.), HBcat (0.2 mmol, 1 equiv.), C_6D_6 (0.5 mL), RT, 30 min. ^{11}B NMR spectroscopic conversion.

The sharp peak associated with **B** can be linked to a change in hybridization of the boron center, from sp^2 to sp^3 .^{41–43} Crystals of compound **B** were isolated by layering a toluene solution of **2a** with a pentane solution of HBcat and confirm the formation of a morpholine dimer bridged by Bcat and BH_2 (Figure 4). Analysis of the crystals by ^1H and ^{11}B NMR spectroscopy shows a mixture containing **B** and **C**, therefore indicating how energetically favored the formation of the decomposition product **C** is.

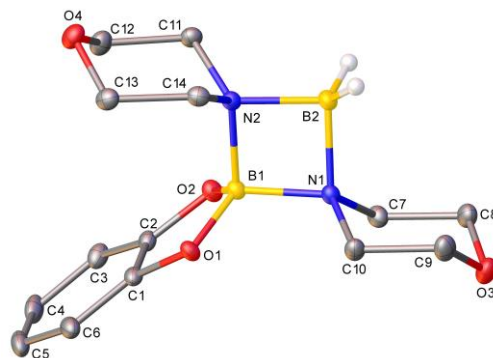


Figure 4. Molecular structure of **B** (CCDC 2263643). Ellipsoids are represented at 30% probability. Hydrogen atoms have been omitted except for those which are bound to boron, for clarity.

The observations from the control reaction between **2a** and HBcat in the presence of **1a**, gives us interesting insight into the mechanism of the reaction. Following formation of **A**, to cleave the Bcat unit and form **B** and **C**, the MePhSiH_2 released from **2a** must act as a hydride transfer agent, cleaving the B–O bond in Bcat and generating a new Si–O bond. Indeed, analysis of the ^1H NMR spectrum of the mixture containing **A**, **B** and **C** shows two directly overlapping quartets at 5.5 ppm and two overlapping doublets at 0.4 ppm corresponding to two sets of shifts for the silicon-centered diastereomers, which are obtained in a 1 : 1 ratio (**D**, Figure 5).

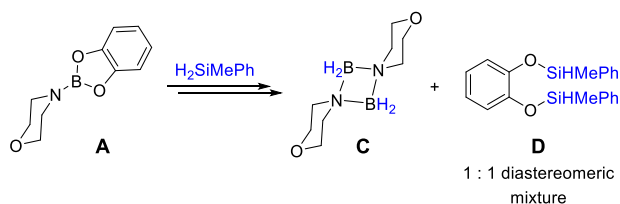


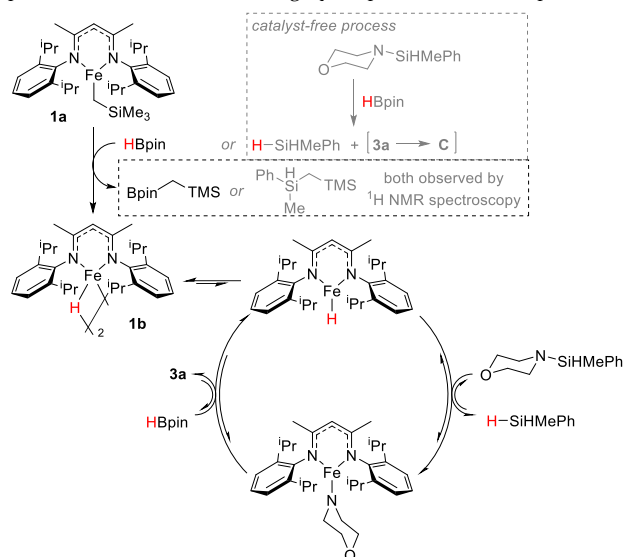
Figure 5. Onward decomposition pathway of **A** to form **C** and **D**.

Although this study did not allow the isolation of analogues of reactive intermediates, it does serve to prove the importance of choice of borane and with this, the importance of catalysis: HBcat undergoes catalyst-free decomposition to form BH_2 -containing products.^{44–47} For HBpin, due to the prolonged reaction time required in the absence of **1a**, decomposition is also observed. Therefore to access Bpin-functionalized amines from silazanes, which have found use recently as amine reagents with enhanced nucleophilicity,^{48–49} catalytic-mediated reactions are key.

Based on the data collected, we postulate the following catalytic cycle (Scheme 6). For pre-catalyst activation, pin BCH_2TMS is observed in the ^{11}B NMR spectra as a new singlet at 34 ppm.^{50–51} This indicates that HBpin is responsible for converting **1a** into **1b**. Noteworthy is the fact that catalyst-free desilylation can occur and thus activation of **1a** to form **1b** can also be afforded by H_2SiMePh , resulting in co-catalytic amounts of both pin BCH_2TMS and $\text{PhMeHSiCH}_2\text{TMS}$ being observed in the ^1H and ^{11}B NMR spectra. This is indeed the case (see SI pages S44 and S47 for details).

In solution, the kinetics obtained via ^1H NMR spectroscopy support that on-cycle, **1b** splits into two active iron-hydride monomers which then mediates catalytic desilylation of the Si–N bond, generating hydrosilane and an iron amido complex which was isolated in the solid-state form as **1c-macrocycle**. To regenerate **1b**, HBpin undergoes σ -bond metathesis, via a non-linear transition state, with **1c** releasing aminoborane **3a** in the process. Stoichiometric reaction of **1c** with HBpin shows instant and clean formation of **1b**, confirming this step in the cycle is viable. H/D scrambling indicates that the steps in the cycle are somewhat reversible. We believe a similar catalytic cycle is

applicable to the depolymerization of polycarbosilazanes and desilylation of silyl ethers. Akin to Nakajima's findings with a bulky Cp'-yttrium catalyst,⁴ the bulky β -diketiminate ligand in our system may be crucial in suppressing the possible degradation pathway of N/O-Bpin product coordination to the highly oxophilic active iron species.



Scheme 6. Proposed catalytic cycle for silazane desilylation with HBpin mediated by **1a**.

CONCLUSION

To summarize, we have employed a well-defined iron β -diketiminate complex and HBpin in the desilylation of silazanes and silyl ethers. Reactions generate free hydrosilane and Bpin-protected amine or alcohol. Reactions of silazanes proceed under mild conditions, often at room temperature, whereas more forcing conditions are required to cleave the Si-O bond in silyl ethers. We have successfully extended our protocol beyond monomeric model compounds, showing the methodology can be used to depolymerize linear and cyclic polycarbosilazanes and poly(silyl ether)s. Our mechanistic investigations allowed the synthesis of an elegant iron β -diketiminate amido hexamer (**1c-macrocycle**), which is active in catalysis, along with an iron-borohydride (**1d**) which is a poor catalyst and clearly a decomposition product generated from BH₃ release⁴⁴⁻⁴⁷ past the end point of catalysis. Based on the data collected we have been able to postulate a credible catalytic cycle.

ASSOCIATED CONTENT

Supporting Information

Synthetic methods, analysis data and NMR spectra for all products is provided in the supporting information (PDF file). The Supporting Information is available free of charge on the ACS Publications website.

AUTHOR INFORMATION

Corresponding Author

* s.kyne@unsw.edu.au

* r.l.webster@bath.ac.uk

Author Contributions

Notes

The authors declare no competing financial interests.

† These authors contributed equally.

ACKNOWLEDGMENT

The University of Bath (MAFJ, AKK, ANB) and EPSRC (DG, SL, RLW) are thanked for funding. Merck is thanked for supply of Durazane polymers. Dr. John Lowe, Dr. Catherine Lyall, Dr. Martin Levere and Dr. Kathryn Proctor are thanked for assistance with analysis.

REFERENCES

- (1) Köhler, T.; Gutacker, A.; Mejía, E., Industrial synthesis of reactive silicones: reaction mechanisms and processes. *Org. Chem. Front.* **2020**, *7*, 4108-4120.
- (2) Lalonde, M.; Chan, T. H., Use of Organosilicon Reagents as Protective Groups in Organic Synthesis. *Synthesis* **1985**, *1985*, 817-845.
- (3) Muzart, J., Silyl Ethers as Protective Groups for Alcohols: Oxidative Deprotection and Stability under Alcohol Oxidation Conditions. *Synthesis* **1993**, *1993*, 11-27.
- (4) Crouch, R. D., Selective deprotection of silyl ethers. *Tetrahedron* **2013**, *69*, 2383-2417.
- (5) Chang, W.-T. T.; Smith, R. C.; Regens, C. S.; Bailey, A. D.; Werner, N. S.; Denmark, S. E. In *Organic Reactions*, pp 213-746.
- (6) Birot, M.; Pillot, J.-P.; Dunogues, J., Comprehensive Chemistry of Polycarbosilanes, Polysilazanes, and Polycarbosilazanes as Precursors of Ceramics. *Chem. Rev.* **1995**, *95*, 1443-1477.
- (7) Abbasi, F.; Mirzadeh, H.; Katbab, A.-A., Modification of polysiloxane polymers for biomedical applications: a review. *Polym. Int.* **2001**, *50*, 1279-1287.
- (8) Abe, Y.; Gunji, T., Oligo- and polysiloxanes. *Prog. Polym. Sci.* **2004**, *29*, 149-182.
- (9) Odian, *Principles of Polymerization*. Wiley: 2004.
- (10) Barroso, G.; Li, Q.; Bordia, R. K.; Motz, G., Polymeric and ceramic silicon-based coatings – a review. *J. Mater. Chem. A* **2019**, *7*, 1936-1963.
- (11) Kumar, V. B.; Leitao, E. M., Properties and applications of polysilanes. *Appl. Organomet. Chem.* **2020**, *34*, e5402.
- (12) Soloducho, J.; Zając, D.; Szychalska, K.; Baluta, S.; Cabaj, J., Conducting Silicone-Based Polymers and Their Application. *Molecules* **2021**, *26*, 2012.
- (13) Armitage, D. A., *Comprehensive Organometallic Chemistry*. Pergamon Press: Oxford, 1982.
- (14) Aoyagi, K.; Matsumoto, K.; Shimada, S.; Sato, K.; Nakajima, Y., Catalytic Reduction of Alkoxysilanes with Borane Using a Metallocene-Type Yttrium Complex. *Organometallics* **2019**, *38*, 210-212.
- (15) Enthaler, S.; Kretschmer, R., Low-Temperature Depolymerization of Polysiloxanes with Iron Catalysis. *ChemSusChem* **2014**, *7*, 2030-2036.
- (16) Enthaler, S., Iron-catalyzed depolymerization of polysiloxanes to produce dichlorodimethylsilane, diacetoxydimethylsilane, or dimethoxydimethylsilane. *J. Appl. Polym. Sci.* **2015**, *132*.

- (17) Weidauer, M.; Heyder, B.; Woelki, D.; Tschiersch, M.; Köhler-Krützfeldt, A.; Enthaler, S., Iron-catalyzed depolymerizations of end-of-life silicones with fatty alcohols. *Resource-Efficient Technologies* **2015**, *1*, 73-79.
- (18) Burg, A. B.; Kuljian, E. S., Silyl-Amino Boron Compounds. *J. Am. Chem. Soc.* **1950**, *72*, 3103-3107.
- (19) Fessenden, R.; Fessenden, J. S., The Chemistry of Silicon-Nitrogen Compounds. *Chem. Rev.* **1961**, *61*, 361-388.
- (20) Dahlhoff, W. V.; Taba, K. M., Boron Compounds; 69. Introduction and Removal of t-Butyldimethylsilyl Groups via Diethylboryloxy Compounds. *Synthesis* **1986**, *1986*, 561-562.
- (21) Stober, M. R.; Michael, K. W.; Speier, J. L., The polymerization of vinylaminosilanes. Unique stability of silicon-nitrogen bonds toward alkyllithium compounds. *J. Org. Chem.* **1967**, *32*, 2740-2744.
- (22) Lorenz, T.; Lik, A.; Plamper, F. A.; Helten, H., Dehydrocoupling and Silazane Cleavage Routes to Organic-Inorganic Hybrid Polymers with NBN Units in the Main Chain. *Angew. Chem. Int. Ed.* **2016**, *55*, 7236-7241.
- (23) Wrackmeyer, B.; Schwarze, B.; Milius, W., Reactions between tetraalkyldiboranes(6) and disilazanes — A convenient route to N-silylamino-dialkylboranes. *J. Organomet. Chem.* **1995**, *489*, 201-205.
- (24) Sharma, H. K.; Pannell, K. H., Activation of the Si-Si Bond by Transition Metal Complexes. *Chem. Rev.* **1995**, *95*, 1351-1374.
- (25) Tahara, A.; Nagino, S.; Sunada, Y.; Haige, R.; Nagashima, H., Syntheses of Substituted 1,4-Disila-2,5-cyclohexadienes from Cyclic Hexasilane Si₆Me₁₂ and Alkynes via Successive Si-Si Bond Activation by Pd/Isocyanide Catalysts. *Organometallics* **2018**, *37*, 2531-2543.
- (26) Oestreich, M.; Hartmann, E.; Mewald, M., Activation of the Si-B Inter-element Bond: Mechanism, Catalysis, and Synthesis. *Chem. Rev.* **2013**, *113*, 402-441.
- (27) Liptrot, D. J.; Arrowsmith, M.; Colebatch, A. L.; Hadlington, T. J.; Hill, M. S.; Kociok-Köhn, G.; Mahon, M. F., Beyond Dehydrocoupling: Group 2 Mediated Boron-Nitrogen Desilacoupling. *Angew. Chem. Int. Ed.* **2015**, *54*, 15280-15283.
- (28) Ohmura, T.; Nishiura, H.; Suginome, M., Palladium-Catalyzed β -Elimination of Aminoboranes from (Aminomethylsilyl)boranes Leading to the Formation of Silene Dimers. *Organometallics* **2017**, *36*, 4298-4304.
- (29) Hayashi, M., Organophosphine syntheses via activation of the phosphorus-silicon bond of silylphosphines. *Chem. Rec.* **2009**, *9*, 236-245.
- (30) King, A. K.; Buchard, A.; Mahon, M. F.; Webster, R. L., Facile, Catalytic Dehydrocoupling of Phosphines Using β -Diketimate Iron(II) Complexes. *Chem. Eur. J.* **2015**, *21*, 15960-15963.
- (31) Coles, N. T.; Mahon, M. F.; Webster, R. L., Phosphine- and Amine-Borane Dehydrocoupling Using a Three-Coordinate Iron(II) β -Diketimate Precatalyst. *Organometallics* **2017**, *36*, 2262-2268.
- (32) Espinal-Viguri, M.; Neale, S. E.; Coles, N. T.; Macgregor, S. A.; Webster, R. L., Room Temperature Iron-Catalyzed Transfer Hydrogenation and Regioselective Deuteration of Carbon-Carbon Double Bonds. *J. Am. Chem. Soc.* **2019**, *141*, 572-582.
- (33) Gasperini, D.; King, A.; Coles, N. T.; Mahon, M. F.; Webster, R. L., Seeking Heteroatom-Rich Compounds: Synthetic and Mechanistic Studies into Iron Catalyzed Dehydrocoupling of Silanes. *ACS Catal.* **2020**, *10*, 6102-6112.
- (34) Sciarone, T. J. J.; Meetsma, A.; Hessen, B., Neutral and cationic Fe(II) β -diketimate complexes. *Inorganica Chimica Acta* **2006**, *359*, 1815-1825.
- (35) Bellini, C.; Orione, C.; Carpentier, J.-F.; Sarazin, Y., Tailored Cyclic and Linear Polycarbosilazanes by Barium-Catalyzed N-H/H-Si Dehydrocoupling Reactions. *Angew. Chem. Int. Ed.* **2016**, *55*, 3744-3748.
- (36) Farcaş-Johnson, M. A.; Kyne, S. H.; Webster, R. L., Dehydrocoupling Polymerization: Poly(silylether) Synthesis by Using an Iron β -Diketimate Catalyst. *Chem. Eur. J.* **2022**, *28*, e202201642.
- (37) Evans, R.; Dal Poggetto, G.; Nilsson, M.; Morris, G. A., Improving the Interpretation of Small Molecule Diffusion Coefficients. *Anal. Chem.* **2018**, *90*, 3987-3994.
- (38) O'Ferrall, R. A. M., Model calculations of hydrogen isotope effects for non-linear transition states. *Journal of the Chemical Society B: Physical Organic* **1970**, 785-790.
- (39) Romero, E. A.; Peltier, J. L.; Jazzar, R.; Bertrand, G., Catalyst-free dehydrocoupling of amines, alcohols, and thiols with pinacol borane and 9-borabicyclononane (9-BBN). *Chem. Commun.* **2016**, *52*, 10563-10565.
- (40) Pasumansky, L.; Haddenham, D.; Clary, J. W.; Fisher, G. B.; Goralski, C. T.; Singaram, B., Lithium Aminoborohydrides 16. Synthesis and Reactions of Monomeric and Dimeric Aminoboranes. *J. Org. Chem.* **2008**, *73*, 1898-1905.
- (41) O'Brien, J. M.; Hoveyda, A. H., Metal-Free Catalytic C-Si Bond Formation in an Aqueous Medium. Enantioselective NHC-Catalyzed Silyl Conjugate Additions to Cyclic and Acyclic α,β -Unsaturated Carbonyls. *J. Am. Chem. Soc.* **2011**, *133*, 7712-7715.
- (42) Ito, H.; Horita, Y.; Yamamoto, E., Potassium tert-butoxide-mediated regioselective silaboration of aromatic alkenes. *Chem. Commun.* **2012**, *48*, 8006-8008.
- (43) Shintani, R.; Fujie, R.; Takeda, M.; Nozaki, K., Silylative Cyclopropanation of Allyl Phosphates with Silylboronates. *Angew. Chem. Int. Ed.* **2014**, *53*, 6546-6549.

- (44) Männig, D.; Nöth, H., Catalytic Hydroboration with Rhodium Complexes. *Angew. Chem. Int. Ed.* **1985**, *24*, 878-879.
- (45) Burgess, K.; Van der Donk, W. A.; Westcott, S. A.; Marder, T. B.; Baker, R. T.; Calabrese, J. C., Reactions of catecholborane with Wilkinson's catalyst: implications for transition metal-catalyzed hydroborations of alkenes. *J. Am. Chem. Soc.* **1992**, *114*, 9350-9359.
- (46) Westcott, S. A.; Blom, H. P.; Marder, T. B.; Baker, R. T., New homogeneous rhodium catalysts for the regioselective hydroboration of alkenes. *J. Am. Chem. Soc.* **1992**, *114*, 8863-8869.
- (47) Westcott, S. A.; Blom, H. P.; Marder, T. B.; Baker, R. T.; Calabrese, J. C., Nucleophile promoted degradation of catecholborane: consequences for transition metal-catalyzed hydroborations. *Inorg. Chem.* **1993**, *32*, 2175-2182.
- (48) Solé, C.; Fernández, E., Alkoxide Activation of Aminoboranes towards Selective Amination. *Angew. Chem. Int. Ed.* **2013**, *52*, 11351-11355.
- (49) Junor, G. P.; Romero, E. A.; Chen, X.; Jazzar, R.; Bertrand, G., Readily Available Primary Aminoboranes as Powerful Reagents for Aldimine Synthesis. *Angew. Chem. Int. Ed.* **2019**, *58*, 2875-2878.
- (50) Ohmura, T.; Torigoe, T.; Suginome, M., Functionalization of Tetraorganosilanes and Permethyloligosilanes at a Methyl Group on Silicon via Iridium-Catalyzed C(sp³)-H Borylation. *Organometallics* **2013**, *32*, 6170-6173.
- (51) Espinal-Viguri, M.; Woof, C. R.; Webster, R. L., Iron-Catalyzed Hydroboration: Unlocking Reactivity through Ligand Modulation. *Chem. Eur. J.* **2016**, *22*, 11605-11608.

